Synthesis and Shape-Tailoring of Copper Sulfide/Indium Sulfide-Based Nanocrystals

Wei Han, Luoxin Yi, Nan Zhao, Aiwei Tang,[†] Mingyuan Gao,* and Zhiyong Tang*,[‡]

Institute of Chemistry, Chinese Academy of Sciences, Bei Yi Jie 2, Zhong Guan Cun, Beijing 100190, China

Received June 25, 2008; E-mail: gaomy@iccas.ac.cn; zytang@nanoctr.cn

Abstract: Heterostructured $Cu_2S-In_2S_3$ nanocrystals with various shapes and compositions were synthesized by a high-temperature precursor-injection method using the semiconductor nanocrystal $Cu_{1.94}S$ as a catalyst. The intrinsic cationic deficiencies formed at high temperature by Cu ions made the $Cu_{1.94}S$ nanocrystal a good candidate for catalyzing the nucleation and subsequent growth of In_2S_3 nanocrystals, eventually leading to the formation of heterostructured $Cu_2S-In_2S_3$ nanocrystals. Gelification of the reaction systems, which were composed of different types of nanocrystal precursors and solvent, was found to be a very effective measure for controlling the growth kinetics of the heterostructured particles. Consequently, matchsticklike $Cu_2S_3-In_2S_3$ heterostructured nanorods, teardroplike quasi-core/shell $Cu_2S@In_2S_3$ nanocrystals, and pencil-like In_2S_3 nanorods were successfully obtained by manipulating the gelification of the reaction system; this formed a solid experimental basis for further discussion of the growth mechanisms for differently shaped and structured nanocrystals. By reaction with 1,10-phenanthroline, a reagent that strongly and selectively binds to Cu^+, a compositional transformation from binary matchsticklike $Cu_2S-In_2S_3$ nanorods to pure In_2S_3 nanorods was successfully achieved.

Introduction

Heterostructured semiconductor devices have proven to be tremendously beneficial for more than half a century,[1] and in the future, heterostructures based on nanometer-sized semiconducting units will undoubtedly lead to revolutionary new applications of nanomaterials in various fields, such as photovoltaic devices,[2] high-performance catalysis,[3] biological and biomedical sensing,[4] and a new generation of optoelectronic devices.[5] Because of quantum-confinement and surface effects, nanometer-sized semiconductors possess unique size-dependent physiochemical properties that one does not see in the corresponding bulk solids.[6] The development of nanometer-sized heterostructured semiconductor materials therefore has great potential for creating new materials with remarkable properties.[7]

To date, two types of synthetic routes have been widely used for creating nano-objects with heterostructures: seeded growth and catalyst-assisted growth.[8] In seeded growth, seeds offer crystallographic facets for the epitaxial growth of the second material, eventually leading to heterostructured nanomaterials. Therefore, a proper lattice mismatch between the growing crystallographic facets of the two different types of nanomaterials is required. Production of dimeric and trimeric nanocrystals with matchsticklike, dumbbell-like, bamboo-like, and branched structures by the seeded-growth method has been reported for various types of material systems, such as metal−metal oxide,[9] metal oxide−semiconductor,[10] metal−metal,[11] metal−semiconductor,[12] and semiconductor−semiconductor sys-

† Institute of Optoelectronic Technology, Beijing JiaoTong University, Beijing 100044, China.
‡ National Center for Nanoscience and Technology, No. 11, Beiyitiao, Zhong Guan Cun, Beijing 100190, China.

(1) (a) Alferov, Z. I. *Semiconductors* **1998**, *32*, 1–14. (b) Ledentsov, N. N.; Ustinov, V. M.; Shchukin, P. S.; Kop'ev, V. A.; Alferov, Z. I. *Semiconductors* **1998**, *32*, 343–365. (c) Kroemer, H. *Rev. Mod. Phys.* **2001**, *73*, 783–793.

(2) (a) Schrier, J.; Demchenko, D. O.; Wang, L.-W.; Alivisatos, A. P. *Nano Lett.* **2007**, *7*, 2377–2382. (b) Kumar, S.; Jones, M.; Lo, S. S.; Scholes, G. D. *Small* **2007**, *3*, 1633–1639. (c) Zhong, H.; Zhou, Y.; Yang, Y.; Yang, C.; Li, Y. *J. Phys. Chem. C* **2007**, *111*, 6538–6543.

(3) (a) Wang, C.; Kwon, K.-W.; Odlyzko, M. L.; Lee, B. H.; Shim, M. *J. Phys. Chem. C* **2007**, *111*, 11734–11741. (b) Liu, J.; Huang, X.; Li, Y.; Sulieman, K. M.; He, X.; Sun, F. *J. Phys. Chem. B* **2006**, *110*, 21865–21872. (c) Kuang, Q.; Jiang, Z.-Y.; Xie, Z.-X.; Lin, S.-C.; Lin, Z.-W.; Xie, S.-Y.; Huang, R.-B.; Zheng, L.-S. *J. Am. Chem. Soc.* **2005**, *127*, 11777–11784. (d) Zheng, Y.; Zheng, L.; Zhan, Y.; Lin, X.; Zheng, Q.; Wei, K. *Inorg. Chem.* **2007**, *46*, 6980–6986.

(4) (a) Gao, J.; Liang, G.; Zhang, B.; Kuang, Y.; Zhang, X.; Xu, B. *J. Am. Chem. Soc.* **2007**, *129*, 1428–1433. (b) Larson, D. R.; Zipfel, W. R.; Williams, R. M.; Clark, S. W.; Bruchez, M. P.; Wise, F. W.; Webb, W. W. *Science* **2003**, *300*, 1434–1436. (c) Choi, J.-S.; Jun, Y.-W.; Yeon, S.-I.; Kim, H. C.; Shin, J.-S.; Cheon, J. *J. Am. Chem. Soc.* **2006**, *128*, 15982–15983. (d) Lee, I. S.; Lee, N.; Park, J.; Kim, B. H.; Yi, Y.-W.; Kim, T.; Kim, T. K.; Lee, I. H.; Paik, S. R.; Hyeon, T. *J. Am. Chem. Soc.* **2006**, *128*, 10658–10659.

(5) (a) Qian, F.; Gradečak, S.; Li, Y.; Wen, C.-Y.; Lieber, C. M. *Nano Lett.* **2005**, *5*, 2287–2291. (b) Thelander, C.; Mårtensson, T.; Björk, M. T.; Ohlsson, B. J.; Larsson, M. W.; Wallenberg, L. R.; Samuelson, L. *Appl. Phys. Lett.* **2003**, *83*, 2052–2054. (c) Gudiksen, M. S.; Lauhon, L. J.; Wang, J.; Smith, D. C.; Lieber, C. M. *Nature* **2002**, *415*, 617–620. (d) Xiang, J.; Lu, W.; Hu, Y.; Wu, Y.; Yan, H.; Lieber, C. M. *Nature* **2006**, *441*, 489–493. (e) Hayden, O.; Agarwal, R.; Lieber, C. M. *Nat. Mater.* **2006**, *5*, 352–356.

(6) Murray, C. B.; Kagan, C. R.; Bawendi, M. G. *Annu. Rev. Mater. Sci.* **2000**, *30*, 545–610.

(7) (a) Cozzoli, P. D.; Pellegrino, T.; Manna, L. *Chem. Soc. Rev.* **2006**, *35*, 1195–1208. (b) Mieszawska, A. J.; Jalilian, R.; Sumanasekera, G. U.; Zamborini, F. P. *Small* **2007**, *3*, 722–756.

(8) (a) Milliron, D. J.; Hughes, S. M.; Cui, Y.; Manna, L.; Li, J.; Wang, L.-W.; Alivisatos, A. P. *Nature* **2004**, *430*, 190–195. (b) Wu, Y.; Fan, R.; Yang, P. *Nano Lett.* **2002**, *2*, 83–86. (c) Ouyang, L.; Maher, K. N.; Yu, C. L.; McCarty, J.; Park, H. *J. Am. Chem. Soc.* **2007**, *129*, 133–138.

tems.[13] In catalyst-assisted growth, including the vapor−liquid−solid (VSL) and the recently developed solution−liquid−solid (SLS) methods,[14] a nanometer-sized particle is used as catalyst for growing nanowires. By successive growth of the second type of material, one-dimensional heterostructures can be obtained. This growing mode requires the following prerequisites: (1) the initial catalyst particle must have a melting point below the reaction temperature; (2) the growing material must have limited solubility in the catalyst particle; and (3) the catalyst particle must not form a solid solution with the growing material.[15] At present, the catalyst particle is exclusively chosen from metals such as Au, Bi, Ga, In, or Sn, Al_xGa_{1-x} alloys, or Au@Bi core/shell-type nanoparticles.[16] In comparison with seeded growth, catalyst-assisted growth is more suitable for preparing heterostructured nano-objects with large aspect ratios.

In_2S_3 is an important n-type semiconductor material that has been widely used in solar cells,[17] color-television picture tubes,[18] and dry cells.[19] In_2S_3 presents both direct and indirect conduction-to-valance transitions.[20] Moreover, the In defects inherent in In_2S_3 allows it to serve as a host for metal ions in forming semiconducting or magnetic materials.[21] In contrast, $Cu_{2-x}S$ is a p-type semiconductor that possesses an x-dependent bandgap energy varying from ∼1.2 eV for chalcocite ($x = 0$) to ∼1.5 eV for digenite ($x = 0.2$) and transforms from an indirect-gap semiconductor to a direct one.[22] Because of these intriguing properties, many recent efforts have been devoted to the synthesis of variously shaped, nanometer-sized $Cu_{2-x}S$ and In_2S_3 materials.[23,24] Further combining these two materials by forming heterostructured nanocrystals would therefore be interesting in regard to achieving special properties, especially in photovoltaic applications.

Pioneering work on preparations of Cu−In sulfide heterostructured nanocrystals with acorn, bottle, and larva shapes has recently been reported.[25] These materials were formed by copyrolyzing Cu−oleate and In−oleate complexes in a mixture of oleylamine and dodecanethiol, and a seed-mediated growth mechanism was proposed for the formation of the heterostructured nanocrystals of various shapes. In our research, through

(9) (a) Zeng, H.; Li, J.; Wang, Z. L.; Liu, J. P.; Sun, S. *Nano Lett.* **2004**, *4*, 187–190. (b) Li, J.; Zeng, H.; Sun, S.; Liu, J. P.; Wang, Z. L. *J. Phys. Chem. B* **2004**, *108*, 14005–14008. (c) Yu, H.; Chen, M.; Rice, P. M.; Wang, S. X.; White, R. L.; Sun, S. *Nano Lett.* **2005**, *5*, 379–382.

(10) (a) Buonsanti, R.; Grillo, V.; Carlino, E.; Giannini, C.; Curri, M. L.; Innocenti, C.; Sangregorio, C.; Achterhold, K.; Parak, F. G.; Agostiano, A.; Cozzoli, P. D. *J. Am. Chem. Soc.* **2006**, *128*, 16953–16970. (b) Kwon, K.-W.; Shim, M. *J. Am. Chem. Soc.* **2005**, *127*, 10269–10275. (c) Gu, H.; Zheng, R.; Zhang, X.; Xu, B. *J. Am. Chem. Soc.* **2004**, *126*, 5664–5665.

(11) (a) Pellegrino, T.; Fiore, A.; Carlino, E.; Giannini, C.; Cozzoli, P. D.; Ciccarella, G.; Respaud, M.; Palmirotta, L.; Cingolani, R.; Manna, L. *J. Am. Chem. Soc.* **2006**, *128*, 6690–6698. (b) Xiang, Y.; Wu, X.; Liu, D.; Jiang, X.; Chu, W.; Li, Z.; Ma, Y.; Zhou, W.; Xie, S. *Nano Lett.* **2006**, *6*, 2290–2294. (c) Ferrer, D.; Torres-Castro, A.; Gao, X.; Sepúlveda-Guzmán, S.; Ortiz-Méndez, U.; José-Yacamán, M. *Nano Lett.* **2007**, *7*, 1701–1705. (d) Chen, J.; Wiley, B.; McLellan, J.; Xiong, Y.; Li, Z.-Y.; Xia, Y. *Nano. Lett.* **2005**, *5*, 2058–2062. (e) Gao, X.; Yu, L.; MacCuspie, R. I.; Matsui, H. *Adv. Mater.* **2005**, *17*, 426–429. (f) Wetz, F.; Soulantica, K.; Falqui, A.; Respaud, M.; Snoeck, E.; Chaudret, B. *Angew. Chem., Int. Ed.* **2007**, *46*, 7079–7081.

(12) (a) Mokari, T.; Rothenberg, E.; Popov, I.; Costi, R.; Banin, U. *Science* **2004**, *304*, 1787–1790. (b) Mokari, T.; Sztrum, C. G.; Salant, A.; Rabani, E.; Banin, U. *Nat. Mater.* **2005**, *4*, 855–863. (c) Pacholski, C.; Kornowski, A.; Weller, H. *Angew. Chem., Int. Ed.* **2004**, *43*, 4774–4777. (d) Carbone, L.; Kudera, S.; Giannini, C.; Ciccarella, G.; Cingolani, R.; Cozzoli, P. D.; Manna, L. *J. Mater. Chem.* **2006**, *16*, 3952–3956. (e) Saunders, A. E.; Popov, I.; Banin, U. *J. Phys. Chem. B* **2006**, *110*, 25421–25429.

(13) (a) Dong, A.; Wang, F.; Daulton, T. L.; Buhro, W. E. *Nano Lett.* **2007**, *7*, 1308–1313. (b) Teranishi, T.; Inoue, Y.; Nakaya, M.; Oumi, Y.; Sano, T. *J. Am. Chem. Soc.* **2004**, *126*, 9914–9915. (c) Talapin, D. V.; Koeppe, R.; Gotzinger, S.; Kornowski, A.; Lupton, J. M.; Rogach, A. L.; Benson, O.; Feldmann, J.; Weller, H. *Nano Lett.* **2003**, *3*, 1677–1681. (d) Shieh, F.; Saunders, A. E.; Korgel, B. A. *J. Phys. Chem. B* **2005**, *109*, 8538–8542. (e) Wang, W.; Lu, X.; Zhang, T.; Zhang, G.; Jiang, W.; Li, X. *J. Am. Chem. Soc.* **2007**, *129*, 6702–6703. (f) Solanki, R.; Huo, J.; Freeouf, J. L.; Miner, B. *Appl. Phys. Lett.* **2002**, *81*, 3864–3866. (g) Dong, A.; Tang, R.; Buhro, W. E. *J. Am. Chem. Soc.* **2007**, *129*, 12254–12262. (h) Björk, M. T.; Ohlsson, B. J.; Sass, T.; Persson, A. I.; Thelander, C.; Magnusson, M. H.; Deppert, K.; Wallenberg, L. R.; Samuelson, L. *Appl. Phys. Lett.* **2002**, *80*, 1058–1060. (i) Kudera, S.; Carbone, L.; Casula, M. F.; Cingolani, R.; Falqui, A.; Snoeck, E.; Parak, W. J.; Manna, L. *Nano Lett.* **2005**, *5*, 445–449. (j) Blackman, B.; Battaglia, D. M.; Mishima, T. D.; Johnson, M. B.; Peng, X. *Chem. Mater.* **2007**, *19*, 3815–3821. (k) Halpert, J. E.; Porter, V. J.; Zimmer, J. P.; Bawendi, M. G. *J. Am. Chem. Soc.* **2006**, *128*, 12590–12591. (l) Robinson, R. D.; Sadtler, B.; Demchenko, D. O.; Erdonmez, C. K.; Wang, L.-W.; Alivisatos, A. P. *Science* **2007**, *317*, 355–358. (m) Xie, R.; Kolb, U.; Basché, T. *Small* **2006**, *2*, 1454–1457. (n) Carbone, L.; et al. *Nano Lett.* **2007**, *7*, 2942–2950. (o) Talapin, D. V.; Nelson, J. H.; Shevchenko, E. V.; Aloni, S.; Sadtler, B.; Alivisatos, A. P. *Nano Lett.* **2007**, *7*, 2951–2959.

(14) (a) Wagner, R. S.; Ellis, W. C. *Appl. Phys. Lett.* **1964**, *4*, 89–90. (b) Trentler, T. J.; Hickman, K. M.; Goel, S. C.; Viano, A. M.; Gibbons, P. C.; Buhro, W. E. *Science* **1995**, *270*, 1791–1794.

(15) Wang, F.; Dong, A.; Sun, J.; Tang, R.; Yu, H.; Buhro, W. E. *Inorg. Chem.* **2006**, *45*, 7511–7521.

(16) (a) Verheijen, M. A.; Immink, G.; Smet, T. D.; Borgstrom, M. T.; Bakkers, E. P. A. M. *J. Am. Chem. Soc.* **2006**, *128*, 1353–1359. (b) Wang, F.; Buhro, W. E. *J. Am. Chem. Soc.* **2007**, *129*, 14381–14387. (c) Ding, Y.; Gao, P. X.; Wang, Z. L. *J. Am. Chem. Soc.* **2004**, *126*, 2066–2072. (d) Yu, H.; Li, J.; Loomis, R. A.; Wang, L.-W.; Buhro, W. E. *Nat. Mater.* **2003**, *2*, 517–520. (e) Pan, Z. W.; Dai, Z. R.; Ma, C.; Wang, Z. L. *J. Am. Chem. Soc.* **2002**, *124*, 1817–1822. (f) Markowitz, P. D.; Zach, M. P.; Gibbons, P. C.; Penner, R. M.; Buhro, W. E. *J. Am. Chem. Soc.* **2001**, *123*, 4502–4511. (g) Grebinski, J. W.; Hull, K. L.; Zhang, J.; Kosel, T. H.; Kuno, M. *Chem. Mater.* **2004**, *16*, 5260–5272.

(17) (a) Dalas, E.; Sakkopoulos, S.; Vitoratos, E.; Maroulis, G.; Kobotiatis, L. *J. Mater. Sci.* **1993**, *28*, 5456–5460. (b) Yu, S.; Shu, L.; Qian, Y.; Xie, Y.; Yang, J.; Yang, L. *Mater. Res. Bull.* **1998**, *33*, 717–721.

(18) Japanese patent application: *Chem. Abstr.* **1981**, *95*, 107324x.

(19) (a) Naghavi, N.; Spiering, S.; Powalla, M.; Cavana, B.; Lincot, D. *Prog. Photovoltaics* **2003**, *11*, 437–443. (b) Sterner, J.; Malmström, J.; Stolt, L. *Prog. Photovoltaics* **2005**, *13*, 179–193.

(20) Nagesha, D. K.; Liang, X.; Mamedov, A. A.; Gainer, G.; Eastman, M. A.; Giersig, M.; Song, J.-J.; Ni, T.; Kotov, N. A. *J. Phys. Chem. B* **2001**, *105*, 7490–7498.

(21) (a) Nakanishi, H. *Jpn. J. Appl. Phys.* **1980**, *19*, 103–108. (b) Becker, R. S.; Zhou, G. D.; Elton, J. *J. Phys. Chem.* **1986**, *90*, 5866–5870. (c) Odenweller, T.; Grabner, E. W. *Ber. Bunsen-Ges. Phys. Chem.* **1988**, *92*, 1330–1334. (d) Kim, D. T.; Yu, K. S.; Kim, W. T. *Sae Mulli* **1991**, *31*, 477–481.

(22) (a) Mulder, B. J. *Phys. Status Solidi A* **1972**, *13*, 79–88. (b) Klimov, V. I.; Karavanskii, V. A. *Phys. Rev. B* **1996**, *54*, 8087–8094.

(23) (a) Reijnen, L.; Meester, B.; Goossens, A.; Schoonman, J. *Mater. Sci. Eng., C* **2002**, *19*, 311–314. (b) Sakamoto, T.; Sunamura, H.; Kawaura, H.; Hasegawa, T.; Nakayama, T.; Aono, M. *Appl. Phys. Lett.* **2003**, *82*, 3032–3034. (c) Klimov, V.; Bolivar, P. H.; Kurz, H.; Karavanskii, V.; Krasovskii, V.; Korkishko, Y. *Appl. Phys. Lett.* **1995**, *67*, 653–655. (d) Sigman, M. B. J.; Ghezelbash, A.; Hanrath, T.; Saunders, A. E.; Lee, F.; Korgel, B. A. *J. Am. Chem. Soc.* **2003**, *125*, 16050–16057. (e) Larsen, T. H.; Sigman, M.; Ghezelbash, A.; Doty, C. R.; Korgel, B. A. *J. Am. Chem. Soc.* **2003**, *125*, 5638–5639. (f) Lim, W. P.; Wong, C. T.; Ang, S. L.; Low, H. Y.; Chin, W. S. *Chem. Mater.* **2006**, *18*, 6170–6177. (g) Zhang, H.-T.; Wu, G.; Chen, X.-H. *Langmuir* **2005**, *21*, 4281–4282. (h) Kuzuya, T.; Yamamuro, S.; Hihara, T.; Sumiyama, K. *Chem. Lett.* **2004**, *33*, 352–353. (i) Chen, L.; Chen, Y.-B.; Wu, L.-M. *J. Am. Chem. Soc.* **2004**, *126*, 16334–16335.

(24) (a) Park, K. H.; Jang, K.; Son, S. U. *Angew. Chem., Int. Ed.* **2006**, *45*, 4608–4612. (b) Tabernor, J.; Christian, P.; O'Brien, P. *J. Mater. Chem.* **2006**, *16*, 2082–2087. (c) Afzaal, M.; Malik, M. A.; O'Brien, P. *Chem. Commun.* **2004**, 334–335. (d) Chen, W.; Bovin, J.-O.; Joly, A. G.; Wang, S.; Su, F.; Li, G. *J. Phys. Chem. B* **2004**, *108*, 11927–11934. (e) Liu, Y.; Xu, H.; Qian, Y. *Cryst. Growth Des.* **2006**, *6*, 1304–1307.

(25) Choi, S.-H.; Kim, E.-G.; Hyeon, T. *J. Am. Chem. Soc.* **2006**, *128*, 2520–2521.

Scheme 1. Synthetic Routes for Preparing (I) Matchsticklike $Cu_2S-In_2S_3$ Heterostructured Nanorods, (II) Teardroplike Quasi-Core/Shell $Cu_2S@In_2S_3$ Nanocrystals, and (III) Pencil-like In_2S_3 Nanorods
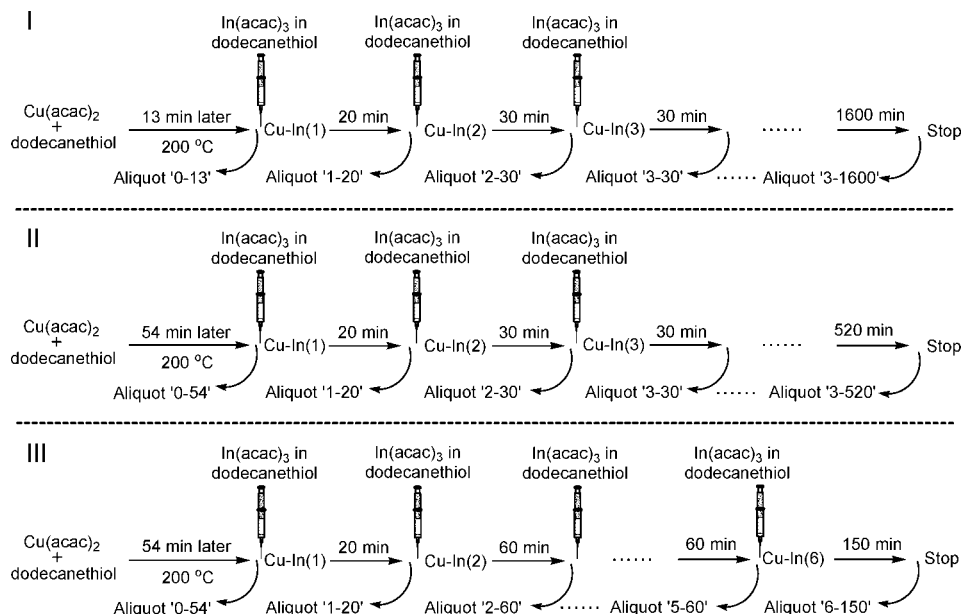
the use of multistep injections of an $In(acac)_3-$dodecanethiol solution into a hot $Cu(acac)_2-$dodecanethiol reaction system without separation and purification of the initially formed copper sulfide nanoparticles, matchsticklike $Cu_2S-In_2S_3$ heterostructured nanorods with a uniform size were successfully obtained. By further careful manipulation of the reaction kinetics, teardroplike quasi-core/shell $Cu_2S@In_2S_3$ nanocrystals as well as pencil-like In_2S_3 nanorods were also produced. Systematic investigations revealed that $Cu_{1.94}S$ nanoparticles formed in the earliest stage of the synthesis served as a catalyst for the subsequent anisotropic growth of the heterostructured nanocrystals. In contrast to the low-melting-point metal nanoparticle catalysts, the intrinsic cationic deficiencies and unusually high cationic mobility of $Cu_{1.94}S$ nanocrystals were believed to be responsible for its ability to catalyze the growth of the Cu_2S/In_2S_3 heterostructured nanocrystals reported herein.

Experimental Section

Materials. Copper(II) acetylacetonate $[Cu(acac)_2]$ and indium(III) acetylacetonate $[In(acac)_3]$ were prepared according to literature methods[26,27] and used after two recrystallizations. 1,10-Phenanthroline trihydrate, *n*-dodecanethiol, and all of the other solvents employed in the current investigations were commercially available analytical-grade products and were used without further purification.

Synthesis of Spherical Copper Sulfide Nanocrystals. The synthesis of the copper sulfide particles was accomplished by directly heating a dodecanethiol solution of $Cu(acac)_2$ under the protection of nitrogen gas. Typically, 0.13 g (0.5 mmol) of $Cu(acac)_2$ powder was dispersed in 30 mL of dodecanethiol with the aid of magnetic stirring, and then nitrogen gas was introduced in order to purge the reaction solution. After ~20 min, the flask containing the sky-blue mixture was quickly immersed in an oil bath at 200 °C. With the increase of temperature, the reaction mixture changed from turbid blue to turbid white. When the temperature reached 148−152 °C, the reaction mixture abruptly turned transparent yellow. Further reaction for ~8 min at 200 °C changed the reaction mixture from transparent yellow to turbid brown, indicating the formation of copper sulfide particles. Aliquots

were extracted during the synthesis for use in monitoring the shape and size evolution of the resultant particles. Typically, the copper sulfide particles were precipitated from aliquots using ethanol as a bad solvent and then collected by centrifugation at 4000 rpm for 10 min. After they were washed twice with chloroform to remove the unreacted precursors and dodecanethiol, the copper sulfide particles were subjected to further characterization.

Synthesis of Matchsticklike $Cu_2S-In_2S_3$ Heterostructured Nanorods. The general preparative procedures are shown in synthetic route I in Scheme 1. First, the copper sulfide nanocrystals were prepared as described above, and then three 3.3 mL portions of dodecanethiol solution, each of which contained 0.07 g (0.17 mmol) of $In(acac)_3$, were intermittently injected into the reaction system without stopping the heating. The first injection was carried out after the reaction for creating copper sulfide nanocrystals had taken place at 200 °C for ~13 min, and the second and third injections were performed 20 and 30 min, respectively, after the ones preceding them. In the final reaction system, the $Cu(acac)_2/In(acac)_3$ molar ratio was ~1:1. The resultant heterostructured nanocrystals were precipitated from aliquots using ethanol and then collected by centrifugation at 4000 rpm for 10 min. After they were washed twice with chloroform to remove the unreacted precursors as well as dodecanethiol, the heterostructured nanocrystals were subjected to further characterization. It should be mentioned that the dodecanethiol solution of $In(acac)_3$ became a gel at room temperature ~15 min after the $In(acac)_3$ powders were dispersed in dodecanethiol. Therefore, the dodecanethiol solutions containing $In(acac)_3$ were always freshly prepared and used before gelification occurred.

Synthesis of Teardroplike Quasi-Core/Shell $Cu_2S@In_2S_3$ Nanocrystals. The preparative procedures for the teardroplike $Cu_2S@In_2S_3$ nanocrystals, which are shown in synthetic route II in Scheme 1, were generally the same as those for the matchsticklike nanocrystals except that the three injections of the $In(acac)_3$ solutions were postponed by ~41 min. The subsequent purification procedures were also the same as those for the matchsticklike nanorods.

Synthesis of Pencil-like In_2S_3 Nanorods. As shown in synthetic route III in Scheme 1, the preparative procedures for the pencil-like In_2S_3 nanorods were the same as those for the teardroplike nanocrystals, except that six (rather than three) injections of equal portions of a 10 mL dodecanethiol solution containing 0.5 mmol

(26) Berg, E. W.; Strassner, J. E. *Anal. Chem.* **1955**, *27*, 127–129.
(27) Morgan, G. T.; Drew, H. D. K. *J. Chem. Soc.* **1921**, *119*, 1058–1066.

of In(acac)$_3$ were made and that after the second injection, a time interval of 60 min (rather than 30 min) between injections was used.

Aliquots extracted at various stages of the preparations described above were labeled as R-*N*-*T*, where R stands for the synthetic route depicted in Scheme 1, *N* designates the number of In(acac)$_3$ portions injected prior to extraction of the aliquot (i.e., *N* = 0 stands for the aliquot extracted right before injection of the first portion, *N* = 1 refers to the aliquot extracted right before injection of the second portion, etc.), and *T* stands for the reaction time (in min) elapsed between the immediately preceding In(acac)$_3$ injection and extraction of the aliquot (or, for *N* = 0, the reaction time used to prepare the initial Cu$_{1.94}$S nanocrystals at 200 °C). This notation is used throughout the paper for all relevant preparations.

Removal of the Cu$_2$S Segment from Matchsticklike Cu$_2$S−In$_2$S$_3$ Nanorods. Removal of the Cu$_2$S segment from the matchsticklike heterostructured nanorods was conducted as follows. The matchsticklike nanorods were collected from a 1 mL aliquot and then redispersed in 3 mL of ethanol, after which 0.23 g (1 mmol) of 1,10-phenanthroline was introduced. The subsequent reaction was allowed to take place at room temperature with magnetic stirring. Aliquots were extracted at different reaction times for monitoring the detachment process.

Control Experiments. In order to explore the formation mechanisms for differently shaped nanocrystals, two additional experiments were carried out. The first experiment was designed to investigate the pyrolysis of In(acac)$_3$ in dodecanethiol. In detail, 0.21 g (0.5 mmol) of In(acac)$_3$ in 30 mL of dodecanethiol was heated to 200 °C and reacted at this temperature for 210 min. In contrast to the Cu(acac)$_2$−dodecanethiol system, the current reaction mixture remained turbid throughout the reaction in spite of the color variation from white to yellow. Moreover, all of the aliquots extracted during the reaction became gels at room temperature. The second control experiment involved simultaneously copyrolyzing equal amounts of Cu(acac)$_2$ (0.13 g, 0.5 mmol) and In(acac)$_3$ (0.21 g, 0.5 mmol) in 30 mL of dodecanethiol at 200 °C. In this system, the reaction mixture changed from turbid white to transparent yellow at ~180 °C and then remained transparent throughout the reaction. Prolonged reaction at 200 °C not only gave rise to a color variation from yellow to red but also weakened the gelification of the reaction system. For example, aliquots extracted within the first 3 h of the reaction became gels at room temperature, whereas such gelification did not occur for aliquots extracted at reaction times longer than 3 h.

Characterization. Low-resolution transmission electron microscopy (TEM) images and selected-area electron diffraction (SAED) patterns were recorded with a JEM-100CXII electron microscope operating at an accelerating voltage of 100 kV. High-resolution TEM (HRTEM) images were taken on FEI Tecnai20 and JEM-2100F microscopes working at an accelerating voltage of 200 kV. Energy-dispersive X-ray spectroscopy (EDXS) was carried out using a GENESIS system (EDAX Inc.) attached to the TEM. For EDXS analysis, the TEM samples were prepared on carbon-coated nickel grids. Statistical sizes of the resultant particles were determined by counting more than 300 nanocrystals per sample. Powder X-ray diffraction (XRD) patterns were obtained with a Regaku D/Max-2500 diffractometer equipped with a Cu Kα$_1$ radiation (λ = 1.54056 Å). Fluorescence and UV−vis absorption spectra were recorded at room temperature with a Cary Eclipse fluorescence spectrometer and a Cary 50 UV−vis spectrometer, respectively.

Results and Discussion

Spherical Cu$_{1.94}$S Nanocrystals. Dodecanethiol was chosen for the preparation of the copper sulfide nanocrystals because it can be used not only as a sulfur precursor[23d,e,g−i] but also as a surface-capping agent. Moreover, its boiling point (266−285 °C) is sufficiently high to enable the thermal decomposition of both Cu(acac)$_2$ and In(acac)$_3$ in the subsequent preparations. It
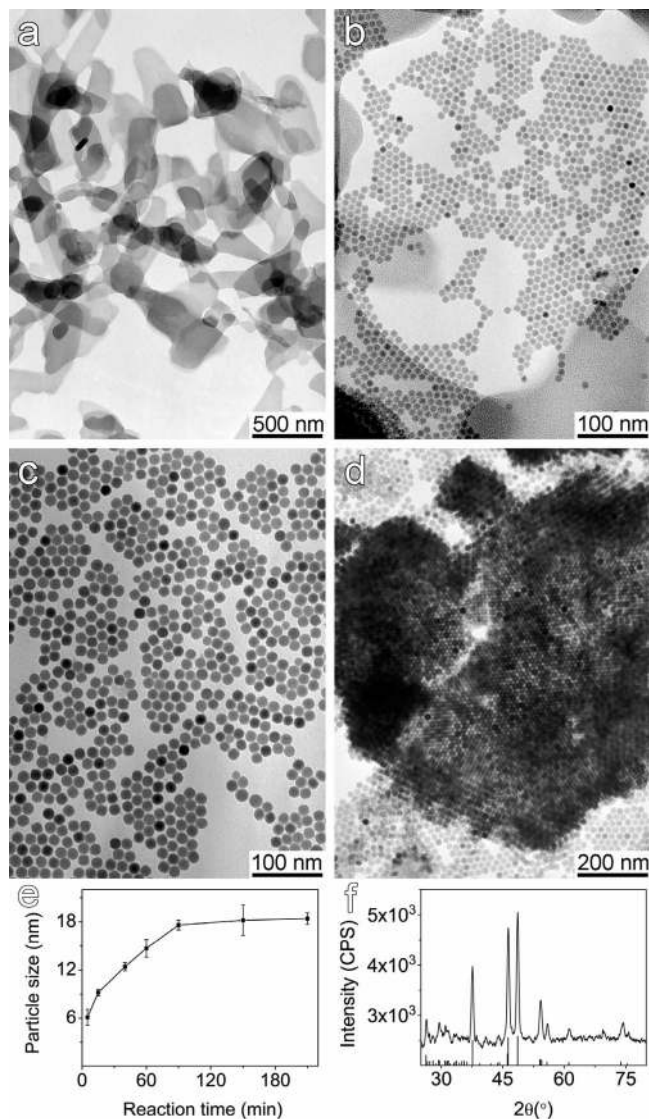

Figure 1. TEM images of samples obtained by pyrolysis of 0.5 mmol of Cu(acac)$_2$ in 30 mL of dodecanethiol at 200 °C for (a) 0, (b) 15, (c) 60, and (d) 210 min. (e) Size evolution of copper sulfide nanocrystals as a function of reaction time at 200 °C. (f) XRD pattern recorded on the sample shown in (d); the lines shown below the pattern are standard data for djurleite (Cu$_{1.94}$S) (JCPDS No. 23-0959).

was found out that the aliquot extracted at 0 min of the reaction at 200 °C became a gel at room temperature. Prolonged reaction gradually changed the color of the reaction mixture from yellow to dark-brown. Meanwhile, the gelification property of the reaction mixture disappeared after 8 min at 200 °C, as shown in Figure S1 in the Supporting Information.

TEM investigations were performed to provide an understanding of the gelification phenomenon and monitor the formation of copper sulfide nanoparticles as well. As shown in Figure 1a, irregularly shaped two-dimensional nanosheets dominantly appeared in the sample extracted after 0 min of reaction at 200 °C. The appearance of these nanostructures, which were self-assembled by coordination polymers formed by dodecanethiol and Cu(acac)$_2$,[28] explains well the gelification phenomenon of the aliquots extracted during the first several minutes of the reaction at 200 °C. However, in the sample extracted 15 min later, most of the lamellar structures were replaced by monodispersed spherical nanoparticles with diam-
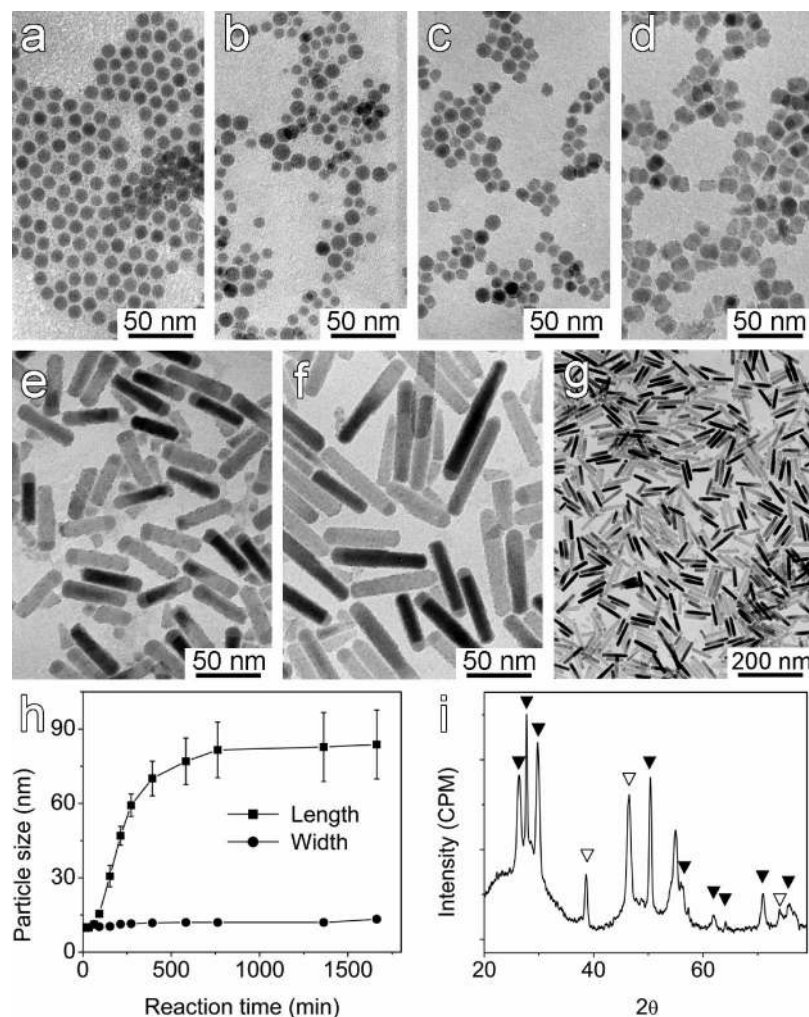
Figure 2. TEM images of samples (a) I-0-13 [extracted right before the injection of the first portion of In(acac)$_3$], (b) I-1-20, (c) I-2-30, (d) I-3-30, (e) I-3-150, and (f, g) I-3-520. (h) Size evolution of nanorods obtained via synthetic route I in Scheme 1. (i) XRD pattern recorded on the sample shown in (g); the solid and hollow triangles indicate the peaks from tetragonal In$_2$S$_3$ (JCPDS No. 73-1366) and hexagonal Cu$_2$S (chalcocite, JCPDS No. 84-0206), respectively.

eters of 10.4 nm, as shown in Figure 1b, indicating that the nanoparticles are formed at the cost of the self-assembled lamellar structures; this conclusion is further supported by the fact that the lamellar structures were completely replaced by larger sulfide nanoparticles at prolonged reaction times (Figure 1c). It should be emphasized that the copper sulfide nanoparticles formed at different reaction times at 200 °C were almost perfectly monodispersed, with a standard deviation less than 5%. Consequently, they readily formed two-dimensional and even three-dimensional superlattice structures, as shown in Figure 1d. The evolution of particle size as a function of reaction time is presented in Figure 1e. The perfect monodispersity of the resultant copper sulfide nanoparticles, which was nearly independent of particle size, was important for effective suppression of the size distribution of the heterostructured nanocrystals formed later.

The crystal structure of the resultant copper sulfide nanoparticles was analyzed by powder XRD. The results shown in

Figure 1f demonstrate that the nanoparticles are crystallized Cu$_{1.94}$S (djurleite, JCPDS No. 23-0959: monoclinic, $a = 26.897$ Å, $b = 15.745$ Å, $c = 13.565$ Å), which possesses a cationic deficiency structure. The mean particle size calculated using the XRD results and the Scherrer equation is ~16.7 nm, which is quite close to the TEM size (18.4 nm) of the same sample, indicating that each individual particle is a single crystal.

Matchsticklike Cu$_2$S−In$_2$S$_3$ Heterostructured Nanorods. As mentioned in the Experimental Section, the matchsticklike Cu$_2$S−In$_2$S$_3$ heterostructured nanorods were prepared by injecting the In(acac)$_3$-dodecanethiol stock solutions into the hot reaction mixture containing the Cu$_{1.94}$S nanocrystals without stopping the heating. The morphological evolution of the Cu$_2$S−In$_2$S$_3$ heterostructured nanorods was monitored by TEM. Representative images recorded from samples I-0-13 [extracted right before the injection of the first portion of In(acac)$_3$], I-1-20, I-2-30, I-3-30, I-3-150, and I-3-520 are shown in Figure 2a−f, respectively, and Figure 2g displays a lower-magnification image of the sample presented in Figure 2f that more clearly shows the uniformity of the heterostructured nanorods. In general, the initial Cu$_{1.94}$S particles were rather monodispersed. However, the monodispersity greatly decreased upon injection of the first portion of the In(acac)$_3$ solution and then slightly

(28) (a) Espinet, P.; Lequerica, M. C.; Martín-Alvarez, J. M. *Chem.−Eur. J.* **1999**, *5*, 1982–1986. (b) Dance, I. G.; Fisher, K. J.; Banda, R. M. H.; Scudder, M. L. *Inorg. Chem.* **1991**, *30*, 183–187. (c) Baena, M. J.; Espinet, P.; Lequerica, M. C.; Levelut, A. M. *J. Am. Chem. Soc.* **1992**, *114*, 4182–4185.
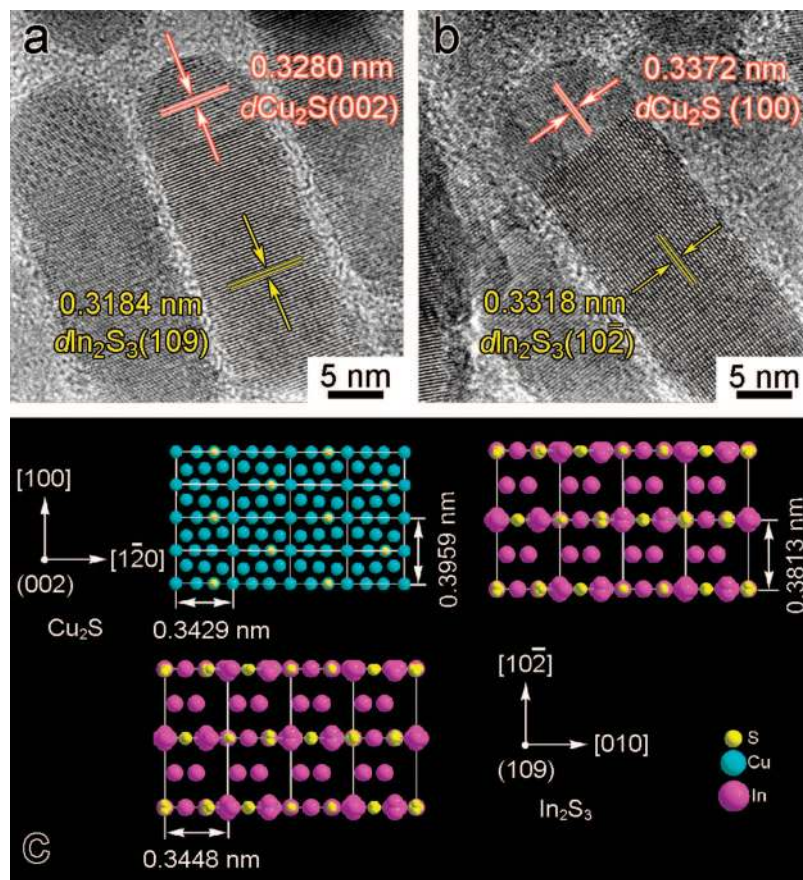
Figure 3. (a, b) HRTEM images of two differently oriented matchsticklike nanorods overlaid with identifications of crystal planes for both Cu_2S and In_2S_3 phases. (c) Schematic model for the atomic arrangements of the epitaxial planes of Cu_2S (002) and In_2S_3 (109), respectively.

recovered until all three portions of In(acac)$_3$ stock solution were completely injected. After that point, another 30 min of reaction at 200 °C led to the formation of Janus-type particles (sample I-3-30 in Figure 2d) that eventually grew into matchsticklike nanorods, as shown in Figures 2e (I-3-150) and 2f,g (I-3-520). Close observation revealed that almost all of the nanorods in Figure 2f were composed of a hemispherical "head" and a rodlike "stick", forming a matchsticklike morphology. The detailed evolution of the length and width of the matchsticklike particles is shown in Figure 2h. Statistical analysis revealed that the average length and width of the nanorods in sample I-3-520 were 77.0 ± 9.4 and 12.0 ± 1.2 nm, respectively. The latter is very close to the diameter of the initial spherical $Cu_{1.94}S$ nanocrystals. XRD measurements (Figure 2i) revealed that the matchsticklike nanorods are made up of tetragonal In_2S_3 (JCPDS No. 73-1366) and copper sulfide having diffraction peaks quite close to those of hexagonal Cu_2S (chalcocite, JCPDS No. 84-0206) rather than $Cu_{1.94}S$, suggesting that the copper sulfide underwent transformations in both crystalline structure and chemical composition (from monoclinic djurleite to hexagonal chalcocite) caused by the growth of the In_2S_3 stick.

In order to show the detailed structure of the junction between the hexagonal Cu_2S head and the tetragonal In_2S_3 stick, HRTEM investigations were performed. An interplanar distance analysis based on the HRTEM image shown in Figure 3a suggested that the In_2S_3 rod epitaxially attaches to the (002) plane of the Cu_2S head through its (109) plane, meaning that the grain boundary is composed of (002) planes of Cu_2S and (109) planes of In_2S_3. Further analysis based on the HRTEM image shown in Figure 3b revealed that the (100) plane of Cu_2S and (10$\bar{2}$) plane of

In_2S_3 are perpendicular to the grain boundary. On the basis of all of these analyses, an atomic packing model that depicts the epitaxial attachment of the tetragonal In_2S_3 stick to the hexagonal Cu_2S head is proposed in Figure 3c. The interface-orientation relationships between the Cu_2S and In_2S_3 are $(1\bar{2}0)_{Cu_2S}\|$-$(010)_{In_2S_3}$ and $(100)_{Cu_2S}\|(10\bar{2})_{In_2S_3}$. The lattice mismatches along these two directions are $[(0.3959 - 0.3813)/0.3959 \times 100\%]$ $= 3.7\%$ and $[(0.3448 - 0.3429)/0.3448 \times 100\%] = 0.6\%$, respectively. The relatively small lattice mismatches along these two directions enable the epitaxial growth of tetragonal In_2S_3 on hexagonal Cu_2S.

Teardroplike Quasi-Core/shell Cu$_2$S@In$_2$S$_3$ Nanocrystals. Interestingly but quite unexpectedly, when the injections of In(acac)$_3$−dodecanethiol solutions were postponed by 41 min (synthetic route II in Scheme 1), the same reaction that produced the matchsticklike $Cu_2S-In_2S_3$ nanorods instead led to uniform teardroplike nanocrystals, as shown in Figure 4a. The average length and width of these "teardrops" were 47.9 ± 4.7 and 22.6 ± 2.4 nm, respectively. HRTEM analysis revealed that the teardrops feature a quasi-core/shell structure composed of a Cu_2S core and a teardroplike In_2S_3 shell (Figure 4b). XRD measurements (data not shown) further confirmed the coexistence of hexagonal Cu_2S and tetragonal In_2S_3 phases in the teardrops.

Growth Mechanism for the Heterostructured Nanocrystals. Up to the present time, the synthesis of semiconductor heterostructures in solution is known to proceed predominantly by either the seeded or catalyst-assisted growth modes. In order to explore the growth mechanism for the current $Cu_2S-In_2S_3$ heterostructured systems, a control experiment involving pyrolysis of only the In(acac)$_3$ precursor in dodecanethiol was conducted in order
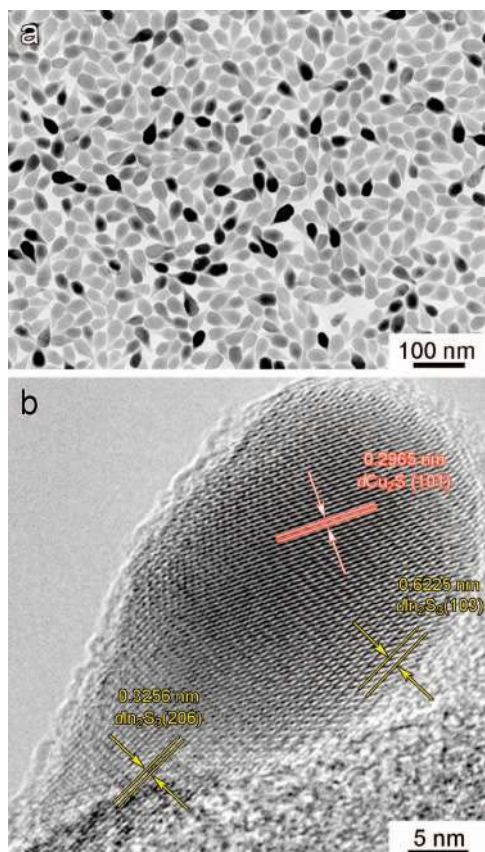
Figure 4. (a) Representative TEM image of teardroplike nanocrystals (II-3-210) obtained via synthetic route II depicted in Scheme 1. (b) HRTEM image of a single teardroplike nanocrystal overlaid with identifications of crystalline phases.
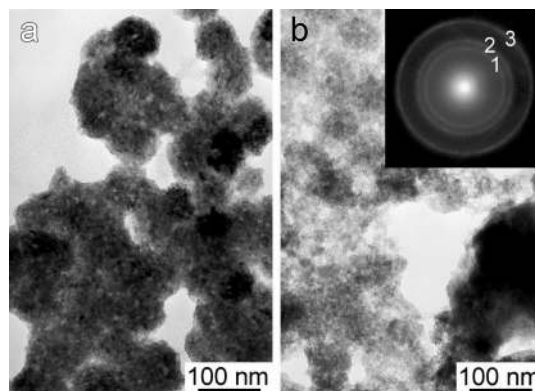

Figure 5. TEM images of samples obtained by pyrolysis of 0.5 mmol of In(acac)$_3$ in 30 mL of dodecanethiol at 200 °C for (a) 30 and (b) 180 min. The *d*-spacing values calculated from the SAED pattern shown in the inset of (b) are 3.266, 2.676, and 1.884 Å, corresponding to the (109), (220), and (400) lattice planes, respectively, of tetragonal In$_2$S$_3$ (JCPDS No. 73-1366).

to discover whether In$_2$S$_3$ nanorods or nanoteardrops could be prepared in the absence of the Cu$_{1.94}$S nanocrystals. In(acac)$_3$ was observed to form gels with dodecanethiol after they were mixed, even at room temperature. Moreover, the gelification property of the In(acac)$_3$–dodecanethiol mixture remained for more than 3 h at 200 °C under stirring (Figure S2 in the Supporting Information), suggesting that In(acac)$_3$ more readily forms coordination polymers with dodecanethiol than Cu(acac)$_2$ does. TEM measurements revealed that the pyrolysis of In(acac)$_3$ in dodecanethiol created only a large number of irregularly shaped aggregates of In$_2$S$_3$ particles (JCPDS No. 73-1366), as shown in Figure 5. These results imply that the Cu$_{1.94}$S nanocrystals promoted the nucleation and subsequent growth of the regularly shaped In$_2$S$_3$ nanocrystals during the formation of the matchsticklike and teardroplike heterostructured particles, possibly via the catalyst-assisted growth method. However, the melting point of bulk Cu$_{1.94}$S is above 1100 °C and is quite unlikely to drop below 200 °C for the nanometer-sized Cu$_{1.94}$S particles. Therefore, the Cu$_{1.94}$S nanocrystals would seem to be an improper choice for catalyzing the growth of In$_2$S$_3$ crystals. Nevertheless, djurleite, as a nonstoichiometric copper sulfide mineral, has only 85% of its copper sites in the hexagonally packed framework of sulfur atoms occupied at temperatures above 125 °C.[29] Moreover, above 100 °C, the Cu atoms in Cu$_{1.94}$S behave virtually like a "fluid", as indicated by djurleite's

unusually large ionic conductivity.[30] All of these intrinsic properties suggest that there will be a large number of copper deficiencies formed in Cu$_{1.94}$S at the current reaction temperature. Therefore, it is reasonable to conclude that Cu$_{1.94}$S served as the catalyst in the formation of the Cu$_2$S–In$_2$S$_3$ heterostructured nanocrystals by working as a host matrix for indium ions, thereby giving birth to In$_2$S$_3$ nanocrystals.

To provide direct evidence for the catalyst-assisted mechanism, the early stages of the morphological evolution of the teardroplike nanocrystals prepared according to synthetic route II in Scheme 1 were investigated by HRTEM. As shown in Figure 6a,A, the initial Cu$_{1.94}$S nanocrystals (II-0-54) appeared as faceted particles. Careful analysis (provided in Figure S3 in the Supporting Information) revealed that these faceted particles were dodecahedrons. However, 20 min after the injection of the first portion of In(acac)$_3$, the faceted Cu$_{1.94}$S nanocrystals lost their initial shape and grew into spherical particles with a Cu$_2$S–In$_2$S$_3$ mixed-crystalline structure (Figure 6b,B). The nanoparticles obtained at this stage (II-1-20) were capped by an amorphous layer that gave rise to an increased particle size of 21.4 ± 1.9 nm. EDXS results (Figure S4 in the Supporting Information) demonstrated that both copper and indium were present in each single particle, further supporting the conclusion that indium was incorporated into the copper sulfide matrix to form the mixed-crystalline structure. However, 30 min after the injection of the second portion of In(acac)$_3$–dodecanethiol solution, the spherical particles were slightly elongated, forming Janus-type heterostructured particles (II-2-30), as shown in Figure 6c,C.

Hereto, the catalyst-assisted growth mechanism rather than the seed-growth mechanism[25] has seemed to be more relevant to the epitaxial growth of In$_2$S$_3$ nanocrystals. In this growth mode, the Cu$_{1.94}$S particle acts as a host in which indium ions occupy its inherent cationic deficiency sites. With an increase in the indium concentration, the highly fluidic nature of the copper ion enables the "supersaturated" indium ion to form an In$_2$S$_3$ phase. Then, as a result of the high interfacial energy, the In$_2$S$_3$ is pushed out of the copper sulfide "embryo" and starts to nucleate on the surface of the Cu$_2$S particle by adopting the

(29) (a) Ueda, R. *J. Phys. Soc. Jpn.* **1949**, *4*, 287–292. (b) Evans, H. T., Jr. *Z. Kristallogr.* **1979**, *150*, 299–320.

(30) (a) Cassaignon, S.; Pauport, T.; Guillemoles, J.-F.; Vedel, J. *Ionics* **1998**, *4*, 364–371. (b) Hirahara, E. *J. Phys. Soc. Jpn.* **1951**, *6*, 428–437.
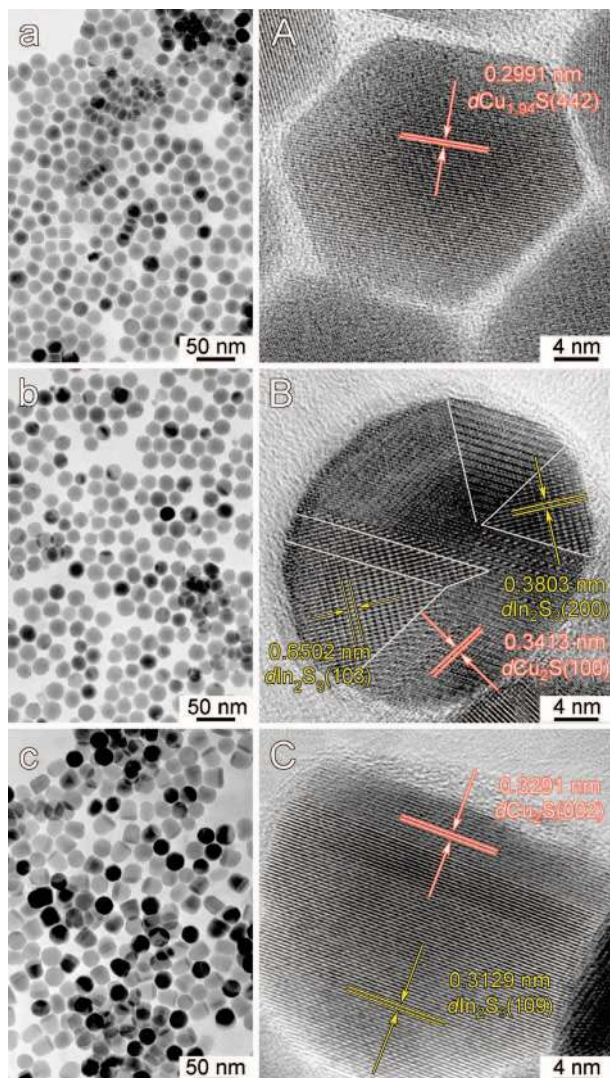
Figure 6. (left) TEM and (right) HRTEM images of samples (a, A) II-0-54, (b, B) II-1-20, and (c, C) II-2-30 obtained via synthetic route II depicted in Scheme 1. Sample II-0-54 was extracted right before the injection of the first portion of In(acac)$_3$.

planes with the smallest crystal-lattice mismatch from the two phases for formation of the grain boundary. Consequently, Janus-type particles are formed, as shown in Figure 6c,C. Similar behavior was reported previously for Ge nanowires prepared by the VLS method using Au nanoparticles as a catalyst.[31]

However, the catalyst-assisted growth mechanism cannot fully explain why the 10.4 nm Cu$_{1.94}$S particles lead to the match-sticklike heterostructure while the 19.7 nm Cu$_{1.94}$S particles give rise to the teardroplike quasi-core/shell heterostructure. Careful experimental observation revealed that the reaction system containing the larger Cu$_{1.94}$S particles gelified at room temperature when the teardroplike particles were formed. In contrast, such gelification was not observed when the matchsticklike nanocrystals were formed. It was previously mentioned that dodecanethiol can form a gel with Cu(acac)$_2$ and that the

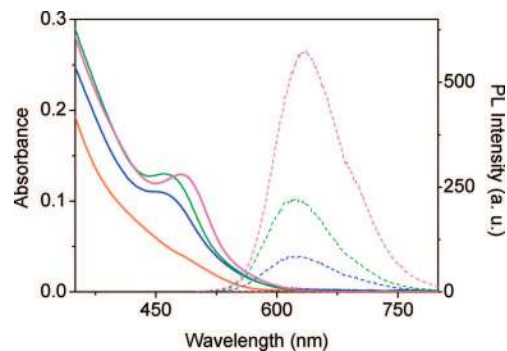gelification phenomenon disappeared after reaction took place for 8 min at 200 °C as a result of deconstruction of the gel network. Although dodecanethiol can also form a gel with In(acac)$_3$, injection of In(acac)$_3$ into the reaction system containing 10.4 nm Cu$_{1.94}$S particles did not generate a gel at any time point during the reaction, suggesting that the presence of a certain amount of an intermediate species that later was converted to Cu$_{1.94}$S nanocrystals, together with the isolated particles (as shown in Figure 2e), prevented In(acac)$_3$ from forming large polymeric structures with dodecanethiol. However, for the larger-particle system, the aliquot containing the teardroplike particles became gelified at room temperature. Since the larger (19.7 nm) Cu$_{1.94}$S particles were obtained upon prolonged pyrolysis of Cu(acac)$_2$, it is reasonable to deduce that the concentration of the Cu(acac)$_2$ precursors in the reaction system was greatly reduced when In(acac)$_3$ was injected. As a result, the amount of In(acac)$_3$ became excessive enough to form a gel network with dodecanethiol after three portions of In(acac)$_3$ had been completely injected, analogous to the simple In(acac)$_3$−dodecanethiol system. The formation of a gel network between In(acac)$_3$ and dodecanethiol would undoubtedly disturb the growth kinetics of the Janus-type particles shown in Figure 6c. As previously mentioned, the In(acac)$_3$−dodecanethiol reaction system can also generate In$_2$S$_3$; consequently, the gelification property of the teardroplike particle system accelerates the condensation of In$_2$S$_3$ on the Cu$_2$S particles. Since the formation of In(acac)$_3$−dodecanethiol coordination polymers can partially extract Cu$^+$ from Cu$_2$S seeds, as supported by the experiments mentioned below, the kinetically controlled fast growing process gives rise to the formation of tailed particles with a quasi core−shell structure. It is important to mention that along with the formation of the teardroplike particles, fluorescent CuInS$_2$ nanocrystals[32] started to appear in the reaction system. Such fluorescent nanoparticles were typically observed by simultaneously pyrolyzing equal amounts of Cu(acac)$_2$ and In(acac)$_3$ in dodecanethiol, as shown in Figure 7 and Figures S5−S7 in the Supporting Information. Therefore, it is reasonable to conclude that the coordination situation between dodecanethiol and indium ions, presented by a nongel/gel transformation of the reaction mixture, strongly influences the growth kinetics of the In$_2$S$_3$ segment in the teardroplike particles. Satisfaction of the gelification accelerates the growth of In$_2$S$_3$ partly at the expense of the copper sulfide seed, eventually leading to the formation of the teardroplike quasi-core/shell nanocrystals.

(31) Wu, Y.; Yang, P. *J. Am. Chem. Soc.* **2001**, *123*, 3165–3166.
(32) (a) Castro, S. L.; Bailey, S. G.; Raffaelle, R. P.; Banger, K. K.; Hepp, A. F. *J. Phys. Chem. B* **2004**, *108*, 12429–12435. (b) Nairn, J. J.; Shapiro, P. J.; Twamley, B.; Pounds, T.; Wandruszka, R. V.; Fletcher, T. R.; Williams, M.; Wang, C.; Norton, M. G. *Nano Lett.* **2006**, *6*, 1218–1223.
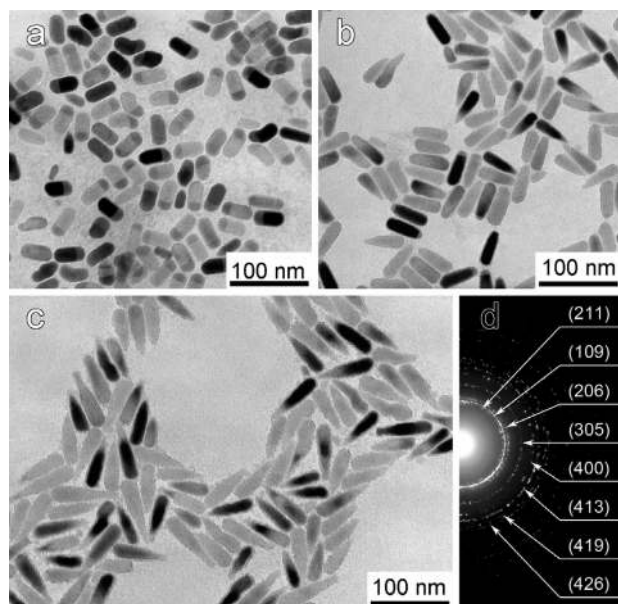
Figure 8. TEM images of samples (a) III-4-60, (b) III-5-60, and (c) III-6-60 obtained via synthetic route III depicted in Scheme 1. (d) SAED pattern of sample III-6-60 together with the identification of diffraction rings labeled with the Miller indices of tetragonal In_2S_3 (JCPDS No. 73-1366).

To further verify that the shape-controlling mechanism for the teardroplike nanocrystals is governed by the gelification property of the reaction system, the following experiments were designed as depicted by synthetic route III in Scheme 1. The preparative procedures were nearly the same as those for the teardroplike nanocrystals (route II), except that the same total amount of $In(acac)_3$ was introduced using six rather than three injections and that after the second injection, the time interval between injections was prolonged from 30 to 60 min. The aim of decreasing the amount of $In(acac)_3$ in each injection and prolonging the interval between injections was to postpone gelification of the reaction mixture. Two important experimental observations should be mentioned here: (1) the aliquot extracted 60 min after the fifth injection of $In(acac)_3$ became gelified at room temperature, and (2) the fluorescent $CuInS_2$ nanocrystals appeared in the aliquot extracted 60 min after the injection of the sixth portion of $In(acac)_3$. Therefore, the samples associated with these two observations were investigated by TEM and HRTEM. As shown in Figure 8a, matchsticklike $Cu_2S-In_2S_3$ nanocrystals (III-4-60) with shorter lengths and larger diameters than those shown in Figure 2g were obtained before the reaction system became gelified. However, when the reaction system became gelified (at room temperature), most of the matchsticks had been "carved" into pencil-like nanocrystals (III-5-60), on some of which a reduced Cu_2S head remained, as shown in Figure 8b. The carving process continued until all of the In_2S_3 particles became pencil-shaped (III-6-60), as shown in Figure 8c. The SAED results shown in Figure 8d demonstrated that the "nanopencils" in Figure 8c were pure tetragonal In_2S_3 (JCPDS No. 73-1366). More details on the morphological evolution of the pencil-like nanocrystals are provided in Figures S8 and S9 in the Supporting Information. The gradual disappearance of the Cu_2S heads and the sharpening of the $Cu_2S-In_2S_3$ sticks starting from the Cu_2S ends, accompanied by the appearance of fluorescent $CuInS_2$ nanocrystals in the reaction system, strongly support the shape-controlling mechanism proposed above, i.e., that the gelification of the reaction
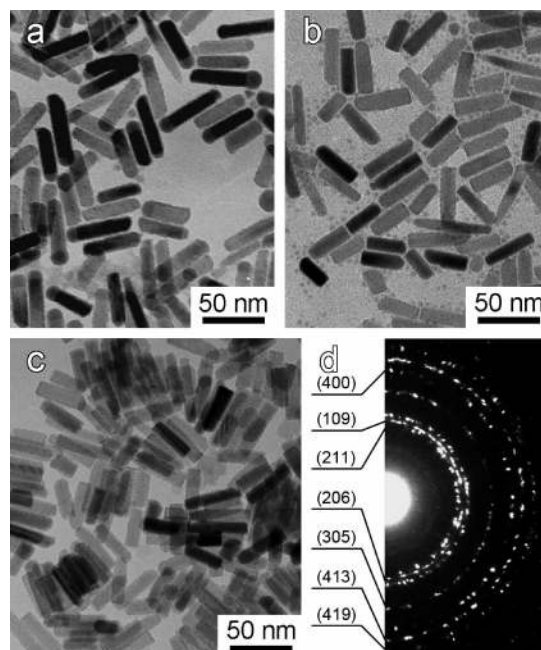
Figure 9. Representative TEM images of matchsticklike $Cu_2S-In_2S_3$ heterostructured nanocrystals obtained after (a) 0, (b) 17, and (c) 51 h of reaction with 1,10-phenanthroline in the Cu_2S-detaching experiment. (d) SAED pattern of the sample in (c) together with the identification of diffraction rings labeled with the Miller indices of tetragonal In_2S_3 (JCPDS No. 73-1366).

system plays a critical role determining the unusual shape of the resultant nanocrystals.

On the basis of all of the above-mentioned results, the growth mechanisms for the teardroplike and pencil-like nanocrystals can be summarized as follows. With respect to the pencil-like particle system, because of the lower concentration of $In(acac)_3$ in the reaction mixture throughout the whole preparative process, resulting from the reduced amount of $In(acac)_3$ in each injection and the longer time interval between injections, the mixed nanocrystals gain enough time to undergo phase separation and subsequently grow in length until the concentration of $In(acac)_3$ becomes high enough to form an $In(acac)_3$−dodecanethiol gel network. As Cu^+ ions from the Cu_2S head of the heterostructured nanocrystals are heavily involved in the formation of coordination polymers, which later produces fluorescent $CuInS_2$ nanocrystals, the growth kinetics of the $Cu_2S-In_2S_3$ heterostructured nanocrystals is strongly disturbed, consequently leading to the formation of sharp tips on the pencil-like In_2S_3 nanocrystals. In contrast, the gelification in the teardroplike particle system comes much earlier, and the higher-concentration burst of $In(acac)_3$ leaves no time for complete detachment of the Cu_2S head from the Janus-type binary nanocrystals (Figure 6c) due to the quick formation of the coordination-polymer network. Consequently, nondirectional deposition of indium on the nanocrystal surface occurs. Simultaneously, In^{3+} ions in the coordination polymer continue to replace Cu^+ ions in Cu_2S segments that are not yet covered by In_2S_3. This replacement process and the subsequent growth of In_2S_3 result in the formation of the tail of the teardrops. Prolonged reaction enables the mixed nanocrystals left within the In_2S_3 shell to undergo phase separation and finally produces the teardroplike quasi-core/shell $Cu_2S@In_2S_3$ nanocrystals.

Shape and Composition Tailoring by Chemical Reaction. In addition to kinetic control of the shape and composition of the

heterostructured nanocrystals, we also attempted to adopt a proper chemical method for realizing these transformations. 1,10-Phenanthroline, known as a common ligand for various types of metal ions, has a much larger binding constant with Cu(I) (log K = 21.05) than with In(III) (log K = 6.20).[33] It was therefore used to detach the Cu_2S head from the matchsticklike nanocrystals. For example, matchsticklike nanocrystals with lengths of 48.9 ± 6.0 nm and widths of 12.0 ± 1.6 nm were used as precursors (Figure 9a). After 17 h of reaction in alcohol, In_2S_3 nanorods with lengths of 38.8 ± 7.1 nm and nearly unchanged rod width (Figure 9b) were obtained. Nevertheless, isolated copper sulfide particles with sizes of 3−4 nm remained abundant in the system until they disappeared when the detaching reaction took place for longer than 50 h (Figure 9c). SAED results demonstrated that the nanorods shown in Figure 9c were pure In_2S_3, identical with those in the heterostructured matchsticks. It should be pointed out that no mature method for the preparation of In_2S_3 nanocrystals with well-defined morphologies has been reported to date. This result exemplifies that by properly selecting a chelating ligand which has different binding constants with cationic ions in a binary nanocrystal, one can realize the shape and composition transformations from the two-component nanocrystal system to a single-component nanocrystal system.

Conclusions

In summary, nearly monodispersed $Cu_{1.94}S$ nanocrystals were produced over a fairly large size range upon the pyrolysis of $Cu(acac)_2$ in dodecanethiol. The intrinsic cationic deficiency in the structure of these $Cu_{1.94}S$ nanocrystals endowed them with the ability to catalyze the growth of In_2S_3 nanocrystals after $In(acac)_3$ in dodecanethiol was injected into the hot reaction system containing $Cu_{1.94}S$ nanocrystals. This eventually led to the formation of differently shaped and structured nanocrystals such as matchsticklike $Cu_2S−In_2S_3$ heterostructured nanorods, teardroplike quasi-core/shell $Cu_2S@In_2S_3$ nanocrystals, and pencil-like In_2S_3 nanorods. Careful observations and systematic investigations revealed that dodecanethiol can coordinate with the metal precursors under proper conditions, leading to the formation of coordination-polymer networks that result in gelification of the reaction system at room temperature. The gelification, as an indicator of the binding situation between the metal precursors and the coordinating solvent dodecanethiol, can therefore be used to manipulate the shape and structure of the resultant nanocrystals, as it greatly alters the growth kinetics of In_2S_3. All of these experimental results suggest that semiconductor $Cu_{1.94}S$ nanocrystals, as a new type of catalyst that differs from the metal nanoparticle catalysts commonly used in the VSL and SLS synthetic routes, will offer new opportunities for growing low-dimensional heterostructured semiconductor nanocrystals via the catalyst-assisted growth mode. Furthermore, as thiol molecules can coordinate with a great number of metal ions, control over the gelification of the reaction system by using thiols may provide a novel route for achieving versatile shape-tailoring for nanomaterials through manipulation of their growth kinetics.

Supporting Information Available: Gelification properties of various reaction systems, morphological analysis of faceted $Cu_{1.94}S$ nanocrystals, EDXS analysis of sample II-1-20, characterization of $CuInS_2$ nanocrystals, temporal evolution of pencil-like nanocrystals prepared according to synthetic route II in Scheme 1, and complete ref 13n. This material is available free of charge via the Internet at http://pubs.acs.org.

JA8046393

(33) (a) Meyer, M.; Albrecht-Gary, A.-M.; Dietrich-Buchecker, C. O.; Sauvage, J.-P. *Inorg. Chem.* **1999**, *38*, 2279–2287. (b) Harrington, J. M.; Oscarson, K. A.; Jones, S. B.; Reibenspies, J. H.; Bartolotti, L. J.; Hancock, R. D. *Z. Naturforsch.* **2007**, *62b*, 386–396.